

Real2Sim2Real: Self-Supervised Learning of Physical Single-Step Dynamic Actions for Planar Robot Casting

Vincent Lim^{1,*}, Huang Huang^{1,*}, Lawrence Yunliang Chen¹, Jonathan Wang¹,
Jeffrey Ichnowski¹, Daniel Seita¹, Michael Laskey², Ken Goldberg¹

Abstract—This paper introduces the task of *Planar Robot Casting (PRC)*: where one planar motion of a robot arm holding one end of a cable causes the other end to slide across the plane toward a desired target. PRC allows the cable to reach points beyond the robot workspace and has applications for cable management in homes, warehouses, and factories. To efficiently learn a PRC policy for a given cable, we propose *Real2Sim2Real*, a self-supervised framework that automatically collects physical trajectory examples to tune parameters of a dynamics simulator using Differential Evolution, generates many simulated examples, and then learns a policy using a weighted combination of simulated and physical data. We evaluate Real2Sim2Real with three simulators, Isaac Gym-segmented, Isaac Gym-hybrid, and PyBullet, two function approximators, Gaussian Processes and Neural Networks (NNs), and three cables with differing stiffness, torsion, and friction. Results with 240 physical trials suggest that the PRC policies can attain median error distance (as % of cable length) ranging from 8% to 14%, outperforming baselines and policies trained on only real or only simulated examples. Code, data, and videos are available at <https://tinyurl.com/robotcast>.

I. INTRODUCTION

Manipulation of deformable objects using a single parameterized dynamic action can be useful for tasks such as fly fishing, lofting a blanket, and playing shuffleboard. Such tasks take as input a desired final state and output one parameterized open-loop dynamic robot action which produces a trajectory toward the final state. This is especially challenging for long-horizon trajectories with complex dynamics involving friction. Although there is substantial research on learning ballistic throwing or hitting motions for rigid objects [30, 67], there is less research into learning dynamic motions to manipulate deformable objects such as cables and fabrics. Dynamics modeling in these contexts is challenging due to uncertainty in deformability, elasticity, and friction during the object’s motion. When computing a single action in this setting (without feedback control), the complexities of state estimation and dynamics modeling are compounded by the long duration for which the system evolves after the robot action. Simulation is often used as an alternative to collecting physical examples, which can be time-consuming and hazardous. However, overcoming the simulation to reality (Sim2Real) gap is a long-standing problem in robotics [20, 32, 41, 54], and is particularly challenging for deformable objects in uncertain dynamic environments.

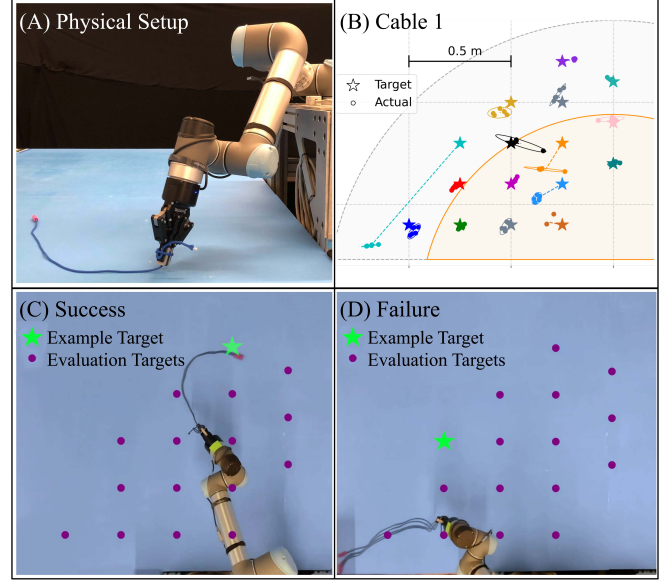


Fig. 1: In *Planar Robot Casting (PRC)*, a single dynamic planar motion of a robot wrist holding one end of a cable causes the other end of the cable to slide across the plane and stop near a desired target point, which may lie outside the robot workspace. (A) shows a side view of a UR5 robot with cable and planar workspace, (B) illustrates test performance on Cable 1 for 5 trials (dots) on 16 targets (stars). The gold inner sector represents the robot workspace, while the grey outer sector represents the reachable workspace of the cable. (C,D) each show five superimposed overhead views of the robot and cable with associated target points after PRC actions with the learned policy, in (C) an example with low error and in (D) an example with high error in endpoint position.

In this paper, we introduce *Planar Robot Casting (PRC)*, where a robot arm dynamically manipulates a cable through 2D space, as illustrated in Fig. 1. We use the generic term *cable* to refer to any 1D deformable object with low stiffness, such as cables, ropes, and threads. We propose *Real2Sim2Real*, a self-supervised robot learning framework that starts by efficiently collecting a small number of physical examples, uses them to tune a simulator, and then uses a combination of physical and simulated examples to train policies for PRC. This paper makes four contributions:

- 1) Real2Sim2Real, a three-step robot learning framework for single-step dynamic actions executed in real environments.
- 2) A formulation of the Planar Robot Casting (PRC) problem, with an automated reset motion and parameterized one-step action space that can reach outside of the reachable area of the robot.
- 3) A physical implementation of PRC using a UR5 robot, and three simulation models of PRC: NVIDIA Isaac

*Equal contribution.

¹The AUTOLab at UC Berkeley (automation.berkeley.edu).

²Toyota Research Institute, CA, USA.

Correspondence to: {vincentklm, huangr}@berkeley.edu

Gym *segmented*, Isaac Gym *hybrid*, and PyBullet. Parameter estimation using Differential Evolution [53, 55] with associated code and datasets from 64,350 simulated experiments and 2,076 physical experiments with 3 distinct cables.

- 4) An application of Real2Sim2Real to PRC, with results suggesting that Real2Sim2Real can efficiently learn PRC control policies that reach target positions within median error of 14% of cable length, even when targets are outside the reachable workspace of the robot.

II. RELATED WORK

A. Deformable 1D Object Manipulation

Manipulation of 1D deformable objects such as cables has a long history in robotics; see Sanchez *et al.* [48] for a recent survey. Some representative applications include surgical suturing [36, 50], knot-tying [6, 17, 37, 58], untangling ropes [16, 29], deforming wires [40], inserting cables into receptacles [52, 59], and playing diabolos [12].

There is recent interest in using learning-based techniques for manipulating cables, often with pick-and-place actions and quasistatic dynamics, so that the robot deforms the cable while allowing it to settle between actions. This can be combined with learning from demonstrations [49, 66] and self-supervised learning [39, 42]. Prior work has also used quasistatic simulators [25] to train cable manipulation policies using reinforcement learning (RL) for transfer to physical robots [60, 65]. However, as we show in Sec. V, there are limits in the free-end reachability of such quasistatic procedures, motivating high-speed, dynamic motions.

B. Simulator Tuning for Sim2Real

Sim2Real transfer has emerged as an effective technique wherein a robot can learn a policy in simulation and transfer it to the real world, which can suffer from the mismatch between simulation and real [20]. One option for Sim2Real is to perform system identification [27] to tune a simulator to match real-world data, but this may be challenging with the infinite-dimensional configuration spaces of cables. An alternative is to use domain randomization over vision [47, 54] or dynamics [43] parameters in simulation. A drawback is that too much randomization can hinder policy training [35] and the randomization range needs to be hand tuned. This has motivated work on interleaving policy training using RL in simulation and tuning simulators with real-world data [9, 13]. Recently, Chang and Padir [8] proposed a Sim2Real2Sim pipeline for cable unplugging where the Sim2Real step determines grasp points, and the Real2Sim step uses sensors to update a cable model in simulation. Similarly, we tune a simulator, but do not require repeated iterations of collecting real-world data with simulator tuning, and we train policies using supervised learning and do not need to use potentially brittle RL algorithms [1, 18]. Unlike Chang and Padir, we do not require cable sensors and we use the tuned simulator to improve the performance of the physical robot.

C. Dynamic Manipulation

In dynamic manipulation, a robot executes rapid actions to move objects to desired configurations [34]. In early work, Lynch and Mason [30] study planar dynamic manipulation primitives such as snatching, throwing, and rolling, and Ruiz-Ugalde *et al.* [46] build a physics-based model of pushing actions so that a robot can slide objects into a desired pose. More recent work has introduced robots that can catch items by predicting item trajectories [21], toss arbitrary objects via self-supervised learning [67], and swing items upwards using tactile feedback [56]. As with these works, we use dynamic motions, but focus specifically on cable manipulation. Furthermore, we use a tuned simulator to accelerate learning and do not require tactile sensing.

D. Dynamic Manipulation of Deformable Objects

Researchers have developed several analytic physics models to describe the dynamics of moving cables. For example, Gatti-Bonoia *et al.* [15] present a 2D dynamic model of fly fishing. They model the fly line as a long elastica and the fly rod as a flexible Euler-Bernoulli beam, and propose a system of differential equations to predict the movement of the fly line in space and time. In contrast to continuum models, Wang *et al.* [57] propose using a finite-element model to represent the fly line by a series of rigid cylinders that are connected by massless hinges. In contrast to these works, we evaluate on physical robots.

For robotic dynamic-cable manipulation, Yamakawa *et al.* [61–64] simplify the modeling of cable deformation by assuming each cable component follows the robot end-effector motion with constant time delay. Kim *et al.* [22] study a mobile robot system with a cable attached as a tail that can strike objects. They use a Rapidly-exploring Random Tree (RRT) [24] and a particle-based representation to address the uncertainty in state transition. In contrast, we aim to control cables for tasks in which we may be unable to rely on assumptions in [22, 62] for cable motion.

In closely related prior work, Zhang *et al.* [68] propose a self-supervised learning technique for dynamic manipulation of fixed-end cables. In contrast, we use free-end cables. Zimmermann *et al.* [69] study the dynamic manipulation of deformable beams and cloth in the free-end setting. They model elastic objects using the finite-element method [4] and use optimal control techniques for trajectory optimization. The simulated motions perform well in real for simple dynamical systems but performance deteriorates for complex soft bodies due to the reality gap. We develop a learned, data-driven approach for robotic manipulation of free-end cables and focus on PRC. Laezza *et al.* [23] develop six customizable benchmark simulation environments for 1D deformable objects, but use an commercial closed-source physics engine. We use easily-accessible physics engines to create dynamic simulation environments.

III. PROBLEM STATEMENT

In Planar Robot Casting, a robot gripper holds a cable at one endpoint and swings it along a planar surface with a

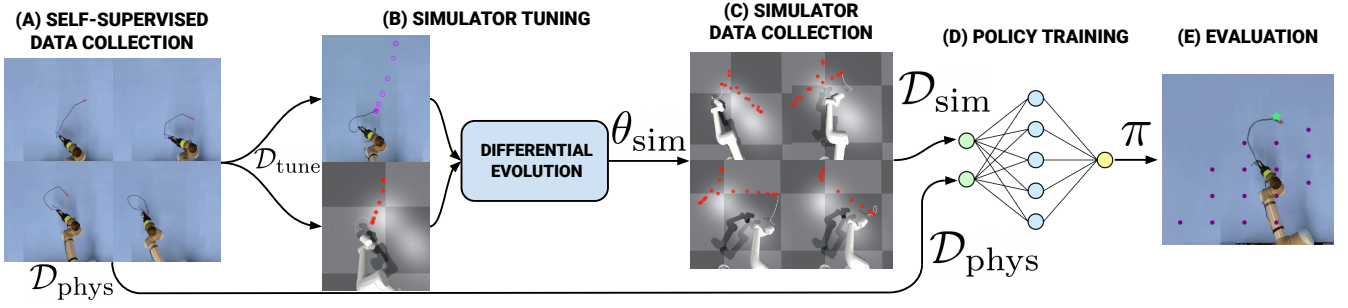


Fig. 2: The *Real2Sim2Real* pipeline for PRC. We collect a physical dataset $\mathcal{D}_{\text{phys}}$ (A) in a self-supervised manner. We subsample $\mathcal{D}_{\text{phys}}$ to generate $\mathcal{D}_{\text{tune}}$, and use it to tune simulation parameters so that its trajectories match real trajectories using Differential Evolution (B), then use the tuned simulator to generate a large dataset \mathcal{D}_{sim} (C). We use a weighted combination of \mathcal{D}_{sim} and $\mathcal{D}_{\text{phys}}$ to train the policy (D) and evaluate the policy in real (E).

single continuous motion so that the other endpoint comes to rest at a target s_d . The held cable endpoint is at polar coordinate $s = (r, \theta)$, with the robot base at the origin. The objective is to find a per-cable policy π that minimizes the expected error $\|s_{f,c} - s_{d,c}\|_2$, where $s_{f,c}$ is the final state and $s_{d,c}$ is s_d in Cartesian coordinates. We assume that the s_d is reachable by the cable endpoint (see Fig. 1).

IV. METHOD

To learn a policy that accounts for variations in cable properties such as mass, stiffness, and friction, we propose the *Real2Sim2Real* (R2S2R) framework (Fig. 2) and apply it to PRC. To support this framework, we define a reset procedure to bring the system into a consistent starting state and a parameterized trajectory function that generates a dynamic arm action. R2S2R first autonomously collects physical trajectories, then tunes a simulator to match the physical environment and generate simulated trajectories. Finally, R2S2R uses a weighted combination of the simulated and physical datasets to train a policy.

A. Reset Procedure

To automate data collection and bring the cable into a consistent starting state before each action, we define a 5-step reset procedure, in which the robot (1) lifts the cable up with the free-end touching the surface to prevent the cable from dangling; (2) continues to lift the cable such that the free-end is just above the surface; (3) hangs still for 3 seconds to stabilize; (4) swings the cable out of the plane, so that the cable straightens along the center axis of the surface and lands with its endpoint far from the robot base; and (5) slowly pulls the cable towards the robot to the reset position $(r_0, 0)$. The reset motion is designed to minimize empirical uncertainty in the reset state, so we assume the start state to be consistent across trajectories. The project website illustrates the reset procedure.

B. Parameterized Actions

To generate quick, smooth, dynamic actions that are low dimensional, thus facilitating data generation and training, we define a parameterized action $\mathbf{a} := (\theta_1, r_1, \theta_2, r_2, \alpha, v_{\text{max}})$ composed of two sweeping arcs (Fig. 3). The motion starts at $(r_0, 0)$, arcs to (r_1, θ_1) , and arcs back to (r_2, θ_2) . In the motion, α is the wrist joint

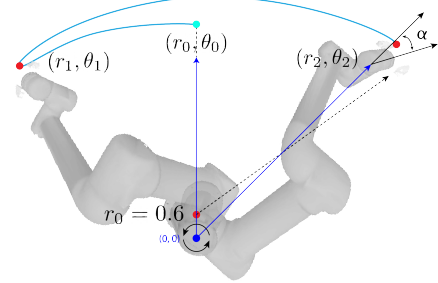


Fig. 3: Example of a spline trajectory traced by the end effector of the UR5 for $r_0 = 0.6$. The reset procedure brings the end effector to $(r_0, 0)$ and the motion is smoothly interpolated along one spline to (r_1, θ_1) , then along a second spline to (r_2, θ_2) . Along the second spline, an offset α is added to the wrist joint angle produced by the IK solver.

rotation about the z -axis during the second arc, and v_{max} is the maximum velocity. This parameterization is motivated by observing human attempts at the PRC task.

We convert action parameters to a trajectory in polar coordinates using a cubic spline to smoothly interpolate the radial coefficient from r_0 to r_2 , and use a maximum-velocity spline to interpolate the angular coefficient from 0 to θ_1 and from θ_1 to θ_2 , with maximum velocity v_{max} . The UR5 has difficulty following high-jerk trajectories, so the maximum-velocity spline uses jerk-limited bang-bang control [19]. We assume a direction change between the two arc motions, so the angular velocity at θ_1 is 0. We use an analytic inverse kinematics (IK) solver to convert the splines to joint configurations. The execution for each trajectory is about 22 seconds, including 20 seconds for the reset motion and 2 seconds for the planar motion.

This parameterization enables state symmetry. For all datasets, we sample actions such that $\theta_1 > 0$, $\theta_2 < 0$, and $\alpha \geq 0$, to obtain targets on the left of the workspace axis of symmetry. If $(\theta_1, \theta_2, r_2, \alpha, v_{\text{max}})$ produces target (r_d, θ_d) , $(-\theta_1, -\theta_2, r_2, -\alpha, v_{\text{max}})$ will produce $(r_d, -\theta_d)$. Thus, we do not evaluate targets on the right of the axis of symmetry.

C. Self-Supervised Physical Data Collection

For the first step of R2S2R, we autonomously collect a physical dataset $\mathcal{D}_{\text{phys}}$ and take a subset of $\mathcal{D}_{\text{phys}}$ to form a simulator tuning dataset $\mathcal{D}_{\text{tune}}$ to perform system identification in simulation (Sec. IV-E). To create $\mathcal{D}_{\text{phys}}$, we grid sample each action parameter to generate $5 \times 5 \times 5 \times 4 \times 2$

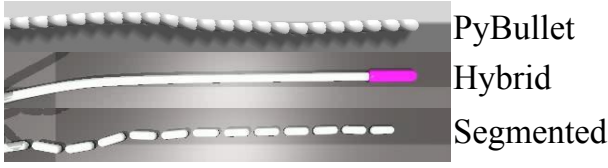


Fig. 4: Three cable simulation models for Real2Sim tuning. From top to bottom: the PyBullet model consists of capsule rigid bodies connected by 6 DOF spring constraints. The hybrid model is a soft-body rod connected to a capsule rigid body at the endpoint. The segmented model also consists of a string of capsule rigid bodies, but is connected using ball joints.

trajectories, then filter out trajectories in collision or exceeding joint limits, to generate $|\mathcal{D}_{\text{phys}}| = 522$ trajectories. Refer to project website for grid sampling details.

For automatic data labeling, we record each trajectory and use OpenCV contour detection [7] to track a brightly colored endpoint. We extract the 2D waypoint location $p_t = (x_t, y_t)$, where t is the timestep, every 100ms from the start of the robot’s trajectory. For each trajectory m_j in $\mathcal{D}_{\text{phys}}$, the number of waypoints collected is $K_j = \lfloor T_j/100 \rfloor$, where T_j is the duration of m_j in milliseconds.

D. Three Simulation Models for Robot Casting

R2S2R then tunes a simulator to generate data to augment policy training. We consider which simulator and model best match real from 3 options: PyBullet [11] and two versions of NVIDIA Isaac Gym [33]. We set simulated cable geometry (e.g., length and radius) to match the real cable. Fig. 4 shows a visual comparison, and the website provides further details.

PyBullet is a CPU-based deterministic rigid-body physics simulator used in prior work on deformable object manipulation [35, 49]. We model the cable as a string of capsule-shaped rigid bodies with 6-DOF spring constraints between each consecutive pair. We tune ten parameters: twist stiffness, bend stiffness, mass, lateral friction, spinning friction, rolling friction, endpoint mass, linear damping, angular damping, and dynamic friction.

NVIDIA Isaac Gym is a GPU-based robotics simulation platform that supports the Flex [31] particle-based physics simulator designed for deformable objects and rigid bodies. We test two simulation models for the cable: a *segmented* model and a *hybrid* model, both using Flex. The segmented model is a string of 18 capsule-shaped rigid bodies with consecutive pairs linked together by a ball joint. To model cable stiffness, we tune the joint friction, cable mass, endpoint mass, and planar friction to capture variation in each respective parameter in real. The hybrid model has the same rigid endpoint from the segmented model, but the rest of the cable is a soft-body rod. We tune the Young’s modulus of the soft-body rod to model both the cable stiffness and elasticity, dynamic friction of the ground plane, and rigid endpoint mass to capture variations in friction and endpoint properties. Simulation environment details are on the website.

E. Simulator Parameter Tuning for \mathcal{D}_{sim} collection

To tune the parameters of each simulator so that simulated and real trajectories closely match, we follow system identification [27] and employ a consistent protocol that

uses physical trajectories from $\mathcal{D}_{\text{tune}}$ (Sec. IV-C) to minimize the discrepancy between simulated and real trajectories. We define the simulation tuning objective as finding simulation parameters that minimize the average L^2 distance between the cable endpoint in simulation \hat{p}_t to the target endpoint p_t over all trajectory timesteps, averaged over a batch of trajectories. We call this metric the average waypoint error.

As the simulation models may have parameters that have no physical analog, such as the joint friction in the segmented model, or have parameters that do not act similarly to their physical counterparts [28], we choose tuning algorithms that make no assumptions about the underlying dynamics model. We evaluate two derivative-free black box optimization algorithms, Bayesian Optimization (BO) and Differential Evolution (DE).

BO builds a probabilistic surrogate model and uses an acquisition function that leverages the uncertainty in the posterior to decide where to query next [14]. BO has been used in policy search for RL hyperparameters [26, 51], and for tuning simulation fluid dynamics [28]. DE is an evolutionary population-based stochastic optimization algorithm widely used for global optimization of nondifferentiable, multimodal, and nonlinear objectives [53]. DE maintains a population of candidate solutions at each iteration and generates new candidates by combining each population member with another mutated population candidate member. It evaluates the fitness of the trial candidates to update the population of candidate solutions until convergence. DE has been shown to be effective at simulation parameter tuning [10].

We evaluate each algorithm via Sim2Sim tests. Using a fixed set of simulation parameters, we generate a small dataset of trajectories to tune randomly initialized simulators to test the effectiveness of DE and BO. We consider the discrepancy between ground truth and predicted simulation parameters and average waypoint error (see results in Sec. V-A). We then tune the simulator parameters for each simulation model to the physical data using the best performing tuning algorithm. We tune the simulator using the same process but with *physical* trajectories from $\mathcal{D}_{\text{tune}}$.

F. Size of Simulator Tuning Set $\mathcal{D}_{\text{tune}}$

We subsample 20 trajectories from $\mathcal{D}_{\text{phys}}$ to generate dataset $\mathcal{D}_{\text{tune}}$. We evaluated whether increasing the size of $\mathcal{D}_{\text{tune}}$ would reduce the discrepancy between simulation and real using a test set of 30 random physical trajectories not in $\mathcal{D}_{\text{phys}}$. We observed negligible difference in test errors between using 20 and 60 trajectories, but the latter require $2\times$ as long to tune on the hybrid and PyBullet models. Tuning with $|\mathcal{D}_{\text{tune}}| = 20$ trajectories did not lead to a significant speedup in the segmented model, therefore we held this value fixed.

After tuning, R2S2R generates training data \mathcal{D}_{sim} by grid sampling θ_1 , θ_2 , r_2 , ψ , and v_{max} to generate $15 \times 15 \times 15 \times 10 \times 2$ values for each respective parameter. We then filter out any trajectories that violate joint limits or with collisions to generate $|\mathcal{D}_{\text{sim}}| = 21,450$ (a, s) simulated trajectories.



Fig. 5: Three cables used in physical experiments. Cable 1 is a thin blue paracord, Cable 2 is a nylon cable, and Cable 3 is a thick jump rope. Each endpoint has an attached mass. The respective cable lengths are 0.63 m, 0.65 m, and 0.65 m, the respective masses are 8 g, 50 g, and 45 g, and the respective radii are 4.5 mm, 10 mm, and 14 mm.

G. Policies

1) *Forward Dynamics Model*: Due to the multi-modality between a target endpoint \mathbf{s} and valid actions \mathbf{a} , we do not learn a policy that directly predicts a given \mathbf{s}_d . Instead, we learn a forward dynamics model f_{forw} that predicts \mathbf{s} given \mathbf{a} , and interpolates to select an action. We parameterize f_{forw} using a fully connected neural network. Given a dataset \mathcal{D} of $(\mathbf{a}, \mathbf{s}_f)$ trajectories, the neural network learns to predict \mathbf{s}_f given \mathbf{a} via standard supervised regression. During evaluation, the policy π grid samples 67,500 input actions \mathbf{a} to form a set \mathcal{A} of candidate actions. It then passes each action through the forward dynamics model f_{forw} , which outputs the predicted endpoint location (\hat{x}, \hat{y}) in Cartesian space. Given a target endpoint \mathbf{s}_d (in polar coordinates), the policy selects the action that minimizes the Euclidean distance between the predicted endpoint \mathbf{s}_f and target endpoint \mathbf{s}_d : $\pi(\mathbf{s}) = \arg \min_{\mathbf{a} \in \mathcal{A}} \|\mathbf{s}_{f,c} - \mathbf{s}_{d,c}\|_2$, where $\mathbf{s}_{f,c}$ and $\mathbf{s}_{d,c}$ are \mathbf{s}_f and \mathbf{s}_d in Cartesian coordinates respectively. Training details can be found on the website.

2) *Baseline Policies*: We consider two alternative policies:

Cast and Pull. Given a target cable endpoint location $\mathbf{s}_d = (r_d, \theta_d)$, the robot rotates θ_d radians and executes a rotated reset motion as in Sec. IV-A, causing the free endpoint to land at (r, θ_d) . The robot then slowly pulls the cable toward the base for a distance of $r - r_d$. The robot arm is limited to a minimum r coordinate of $r_{\min} = 0.55$ to prevent the end effector from hitting the robot’s supporting table, where r_{\min} is the distance from the center of the robot base to the edge of the table, limiting the reachable workspace.

Forward Dynamics Model using Gaussian Process. As a learning baseline, we train a GP regressor [38, 45] using $\mathcal{D}_{\text{phys}}$ to predict the cable endpoint location \mathbf{s}_f given input action \mathbf{a} . As with the neural network forward dynamics model, we grid sample 67,500 input actions and select the trajectory that minimizes the predicted Euclidean distance to the target. We do not train a GP regressor using the simulated dataset as GP regression becomes intractable for large datasets with thousands of datapoints [5].

V. EXPERIMENTS

We evaluate the R2S2R pipeline on PRC with 3 cables (Fig. 5) using a UR5 robot (Fig. 1). The working surface is a 2.45 m wide and 1.55 m tall masonite board, painted blue and sanded to create a consistent friction coefficient across the surface. We use an overhead Logitech Brio 4K webcam recording 1920×1080 images at 60 frames per second.

We consider three forward dynamics model policies:

Sim. Model	Cable 1		Cable 2		Cable 3	
	Wayp.	Last	Wayp.	Last	Wayp.	Last
PyBullet	29%	28%	28%	28%	23%	17%
Isaac Gym Hybrid	14%	23%	11%	14%	11%	13%
Isaac Gym Segm.	9%	13%	8%	9%	11%	13%

TABLE I: Error for simulators tuned using DE on a set of 30 test trajectories for 3 cables (see Fig. 5). The two metrics are the median final L^2 -distance, which is the 2D Euclidean distance between endpoint locations in simulation and reality after a trajectory terminates, and average waypoint (“Wayp.”) error. Values are expressed in percentages of cable length.

- 1) π_{RD} , trained on a small real dataset $\mathcal{D}_{\text{phys}}$.
- 2) π_{SD} , trained on a large simulated dataset \mathcal{D}_{sim} .
- 3) π_{R2S2R} , trained on the combined dataset $\mathcal{D}_{\text{phys}} \cup \mathcal{D}_{\text{sim}}$.

Since $|\mathcal{D}_{\text{sim}}| \gg |\mathcal{D}_{\text{phys}}|$, we 1) upsample $\mathcal{D}_{\text{phys}}$ by randomly duplicating samples such that the real data make between 30% and 40% of the combined dataset to force the model to learn more from the real data, and 2) weight the loss function so that samples from $\mathcal{D}_{\text{phys}}$ are weighted higher. We empirically choose the upsampling percentage and real sample weights to be the best performing values.

A. Comparing Real2Sim Tuning Methods

To test the effectiveness of BO and DE for tuning the Isaac Gym simulators, we generate simulated data for several hybrid models and segmented models with arbitrarily chosen parameters. We then apply BO and DE to tune the respective simulator model parameters. For BO, we use the GPyOpt [3] library, and test three acquisition functions: Expected Improvement (EI), Lower Confidence Bound (LCB), and Maximum Probability of Improvement (MPI). We use DE as implemented in SciPy [55]. With 5 tuning trajectories, EI performs better than LCB and MPI. The tuning errors using BO range from 3.39% to 17.98% for the hybrid model and 1.09% to 9.25% for the segmented model. DE consistently tunes the parameters to within 1% of the ground truth parameters for both the hybrid and segmented models, thus we use DE for all further simulator tuning results.

B. Real2Sim

Table I reports the Real2Sim simulator tuning results using DE. We observe that the segmented model consistently outperforms the PyBullet and hybrid models in minimizing the discrepancy between simulation and real. For the hybrid model, We find that the tuning algorithms reduce the value of Young’s modulus to decrease cable stiffness, but also increases the stretchiness along the length of the cable, which we did not observe in real. We attribute the PyBullet model performance to spring-system simulation instability associated with high spring forces, particularly when preventing the cable from stretching along the length of the cable.

For cable 3, we observe that the hybrid and segmented models perform similarly. Since cable 3 is stiffer, DE produces higher Young’s modulus values that both make the simulated cable stiffer and cause it to stretch less along its length, both of which are desired properties.

While the errors for cable 2 are below 10%, we observe that cables 1 and 3 are harder for each simulator to model,

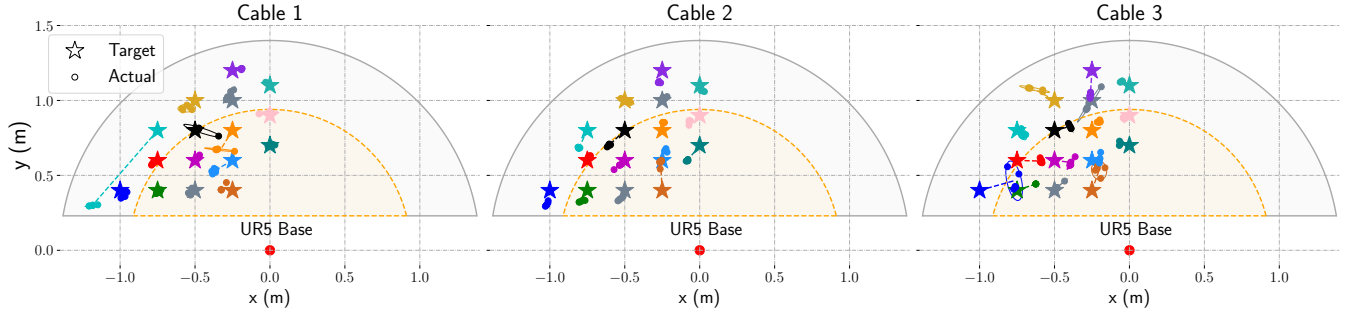


Fig. 6: Evaluation results for π_{R2S2R} for each cable. The inner orange shaded region represents the robot workspace and the outer grey shaded region represents the cable workspace. The colored stars and dots represent each of 16 target locations and resulting endpoints for 5 trials per target respectively, with associated 95% confidence ellipses. The dashed lines connect the center of each ellipse to the target location representing the mean error in position.

Model	Dataset	Median	Q_1	Q_3	Min	Max
Cast and Pull	N/A	61%	38%	86%	6%	124%
Gaussian Proc.	\mathcal{D}_{phys}	27%	9%	51%	4%	97%
π_{RD}	\mathcal{D}_{phys}	15%	11%	21%	8%	36%
π_{SD}	\mathcal{D}_{sim}	14%	10%	17%	6%	115%
π_{R2S2R}	$\mathcal{D}_{phys} \cup \mathcal{D}_{sim}$	8%	5%	12%	2%	105%

TABLE II: Physical evaluation results on Cable 1 of the 2 baselines and the dynamics model f_{forw} trained on three different datasets over a total of $16 \times 5 = 75$ trials. Q_1 and Q_3 are the first and third quartile. All errors are expressed as a percentage of cable length (0.65 m).

Cable	Median	1st Quartile	3rd Quartile	Min	Max
Cable 1	8%	5%	12%	2%	105%
Cable 2	12%	8%	16%	4%	28%
Cable 3	14%	9%	23%	6%	38%

TABLE III: Physical evaluation results using π_{R2S2R} of 3 cables (see Fig. 5) on 16 target locations with 5 trials each per cable for a total of 75 trials using policies trained according to π_{R2S2R} . All errors are expressed as percentages of cable length.

each with a 4% higher last endpoint error for the segmented model. This may be due to plastic deformation in cables 1 and 3, as we observed that slight bends in the cables would remain until manually straightened by a human operator. We generate \mathcal{D}_{sim} using the segmented model, which requires approximately 4.5 minutes using 4 NVIDIA V100s.

C. Physical Experiments

As summarized in Table II, we evaluate two baseline policies and PRC policies π_{RD} , π_{SD} , π_{R2S2R} on cable 1.

1) *Baseline Policies*: The analytic “Cast and Pull” baseline performs the worst out of any of the policies, as the robot would collide with the base for targets near the base. The GP trained on \mathcal{D}_{phys} has substantially worse median, 3rd quartile, and maximum errors, but slightly outperforms π_{RD} in minimum and 1st quartile errors.

2) *Forward Dynamics Models*: We find that policies π_{RD} and π_{SD} have similar median and first and third quartile errors, but π_{SD} has a substantially higher maximum error, corresponding to trajectories where the simulator has high tuning error. As the simulator is tuned with only 20 trajectories, compared to the over 500 trajectories used to train π_{RD} , we achieve similar evaluation performance while using 96% fewer physical trajectories. When we combine the two datasets to train π_{R2S2R} , the median error drops by nearly 50%. The maximum error rose to above 100% for a single

target, suggesting that while the combined dataset substantially improves overall results, it may introduce outliers in regions of the workspace with high reality gap. Given that π_{R2S2R} performs the best out of the policies, we proceed to evaluate the performance for 3 cables on 16 target positions using policy π_{R2S2R} trained for each cable separately, and repeat each action 5 times per target. Results are summarized in Table III. We quantify the aleatoric uncertainty with the 95% confidence ellipses in Fig. 6.

We attribute the epistemic uncertainty to two sources: the Sim2Real gap, where trajectories executed in simulation do not accurately reflect real, and the learning error in the forward dynamics model. The results suggest that the R2S2R pipeline can apply to other cables.

VI. CONCLUSION AND FUTURE WORK

In this paper, we present Real2Sim2Real, a self-supervised learning framework, and apply it to Planar Robot Casting. Experiments suggest that the framework, which collects physical data, tunes a simulator to match the real data, and trains policies from a weighted combination of real and simulated data, can achieve a median error between 12% and 15% of cable length on the PRC task.

As motion is restricted to a 2D plane, we do not address the 3D analog of PRC, Spatial Robot Casting (SRC), used in tasks such as fly fishing [15]. PRC is easier to visualize than SRC but can be harder to model due to inherent uncertainty about static and dynamic friction. In both PRC and SRC, the cable is infinite-dimensional and there is a long time horizon for the motion of the cable free end resulting from a motion at the controlled end.

In future work, we will explore alternate Real2Sim and Sim2Real techniques [2, 13, 43, 44] and apply Real2Sim2Real to other tasks such as grasping and fabric manipulation.

ACKNOWLEDGMENTS

This research was performed at the AUTOLAB at UC Berkeley in affiliation with the Berkeley AI Research (BAIR) Lab and the CITRIS “People and Robots” (CPAR) Initiative. The authors were supported in part by the Toyota Research Institute. We thank our colleagues Justin Kerr, Alejandro Escontrela, Ashwin Balakrishna, Ellen Novoseller, Brijen Thananjeyan, Harry Zhang, Zachary Tam, Chung Min Kim, and Ananth Rao for helpful comments.

REFERENCES

- [1] J. Achiam, *Spinning Up in Deep Reinforcement Learning*, 2018.
- [2] A. Allevato, E. S. Short, M. Pryor, and A. Thomaz, “Tunenet: One-shot residual tuning for system identification and sim-to-real robot task transfer,” in *Conference on Robot Learning*, PMLR, 2020, pp. 445–455.
- [3] T. G. authors, *Gpyopt: A bayesian optimization framework in python*, <http://github.com/SheffieldML/GPyOpt>, 2016.
- [4] K. Bathe, *Finite Element Procedures*. Prentice Hall, 2006.
- [5] M. Belyaev, E. Burnaev, and Y. Kapushev, “Exact inference for gaussian process regression in case of big data with the cartesian product structure,” *arXiv preprint arXiv:1403.6573*, 2014.
- [6] J. van den Berg, S. Miller, D. Duckworth, H. Hu, A. Wan, X.-Y. Fu, K. Goldberg, and P. Abbeel, “Superhuman Performance of Surgical Tasks by Robots Using Iterative Learning from Human-Guided Demonstrations,” in *IEEE International Conference on Robotics and Automation (ICRA)*, 2010.
- [7] G. Bradski, “The OpenCV Library,” *Dr. Dobb’s Journal of Software Tools*, 2000.
- [8] P. Chang and T. Padi, “Sim2Real2Sim: Bridging the Gap Between Simulation and Real-World in Flexible Object Manipulation,” in *IEEE International Conference on Robotic Computing (IRC)*, 2020.
- [9] Y. Chebotar, A. Handa, V. Makoviychuk, M. Macklin, J. Issac, N. Ratliff, and D. Fox, “Closing the Sim-to-Real Loop: Adapting Simulation Randomization with Real World Experience,” in *IEEE International Conference on Robotics and Automation (ICRA)*, 2019.
- [10] J. Collins, R. Brown, J. Leitner, and D. Howard, “Traversing the Reality Gap via Simulator Tuning,” *arXiv preprint arXiv:2003.01369*, 2020.
- [11] E. Coumans and Y. Bai, *PyBullet, a Python Module for Physics Simulation for Games, Robotics and Machine Learning*, <http://pybullet.org>, 2021.
- [12] F. von Drigalski, D. Joshi, T. Murooka, K. Tanaka, M. Hamaya, and Y. Ijiri, “An Analytical Diabolo Model for Robotic Learning and Control,” *arXiv preprint arXiv:2011.09068*, 2020.
- [13] Y. Du, O. Watkins, T. Darrell, P. Abbeel, and D. Pathak, “Auto-Tuned Sim-to-Real Transfer,” in *IEEE International Conference on Robotics and Automation (ICRA)*, 2021.
- [14] P. I. Frazier, “A tutorial on bayesian optimization,” *arXiv preprint arXiv:1807.02811*, 2018.
- [15] C. Gatti-Bono and N. Perkins, “Numerical Model for the Dynamics of a Coupled Fly Line / Fly Rod System and Experimental Validation,” *Journal of Sound and Vibration*, 2004.
- [16] J. Grannen, P. Sundaresan, B. Thananjeyan, J. Ichnowski, A. Balakrishna, M. Hwang, V. Viswanath, M. Laskey, J. E. Gonzalez, and K. Goldberg, “Untangling Dense Knots by Learning Task-Relevant Keypoints,” in *Conference on Robot Learning (CoRL)*, 2020.
- [17] J. Hopcroft, J. Kearney, and D. Kraft, “A Case Study of Flexible Object Manipulation,” in *International Journal of Robotics Research (IJRR)*, 1991.
- [18] J. Ibarz, J. Tan, C. Finn, M. Kalakrishnan, P. Pastor, and S. Levine, “How to Train Your Robot with Deep Reinforcement Learning: Lessons we Have Learned,” in *International Journal of Robotics Research (IJRR)*, 2021.
- [19] J. Ichnowski, Y. Avigal, V. Satish, and K. Goldberg, “Deep learning can accelerate grasp-optimized motion planning,” *Science Robotics*, vol. 5, no. 48, 2020.
- [20] N. Jakobi, P. Husbands, and I. Harvey, “Noise and the Reality Gap: The use of Simulation in Evolutionary Robotics,” in *European Conference on Advances in Artificial Life*, 1995.
- [21] S. Kim, A. Shukla, and A. Billard, “Catching Objects in Flight,” *IEEE Transactions on Robotics*, vol. 30, no. 5, pp. 1049–1065, 2014.
- [22] Y.-H. Kim and D. A. Shell, “Using a Compliant, Unactuated Tail to Manipulate Objects,” in *IEEE Robotics and Automation Letters (RA-L)*, 2016.
- [23] R. Laezza, R. Gieselmann, F. T. Pokorny, and Y. Karayiannidis, “Reform: A robot learning sandbox for deformable linear object manipulation,” in *2021 IEEE International Conference on Robotics and Automation (ICRA)*, 2021, pp. 4717–4723.
- [24] S. M. LaValle and J. J. Kuffner, “Randomized Kinodynamic Planning,” in *International Journal of Robotics Research (IJRR)*, 2001.
- [25] X. Lin, Y. Wang, J. Olkin, and D. Held, “SoftGym: Benchmarking Deep Reinforcement Learning for Deformable Object Manipulation,” in *Conference on Robot Learning (CoRL)*, 2020.
- [26] D. J. Lizotte, T. Wang, M. H. Bowling, D. Schuurmans, et al., “Automatic gait optimization with gaussian process regression,” in *IJCAI*, vol. 7, 2007, pp. 944–949.
- [27] L. Ljung, *System Identification: Theory for the User*. USA: Prentice-Hall, Inc., 1986.
- [28] T. Lopez-Guevara, R. Pucci, N. K. Taylor, M. U. Gutmann, S. Ramamoorthy, and K. Suhr, “Stir to pour: Efficient calibration of liquid properties for pouring actions,” in *2020 IEEE/RSJ International Conference on Intelligent Robots and Systems (IROS)*, 2020, pp. 5351–5357.
- [29] W. H. Lui and A. Saxena, “Tangled: Learning to Untangle Ropes with RGB-D Perception,” in *IEEE/RSJ International Conference on Intelligent Robots and Systems (IROS)*, 2013.
- [30] K. M. Lynch and M. T. Mason, “Dynamic nonprehensile manipulation: Controllability, planning, and experiments,” *The International Journal of Robotics Research*, vol. 18, no. 1, pp. 64–92, 1999.
- [31] M. Macklin, M. Muller, N. Chentanez, and T.-Y. Kim, “Unified Particle Physics for Real-Time Applications,” *ACM Trans. Graph.*, vol. 33, no. 4, Jul. 2014.
- [32] J. Mahler, J. Liang, S. Niyaz, M. Laskey, R. Doan, X. Liu, J. A. Ojea, and K. Goldberg, “Dex-Net 2.0: Deep Learning to Plan Robust Grasps with Synthetic Point Clouds and Analytic Grasp Metrics,” in *Robotics: Science and Systems (RSS)*, 2017.
- [33] V. Makoviychuk, L. Wawrzyniak, Y. Guo, M. Lu, K. Storey, M. Macklin, D. Hoeller, N. Rudin, A. Allshire, A. Handa, and G. State, *Isaac Gym: High Performance GPU-Based Physics Simulation For Robot Learning*, 2021. [arXiv: 2108.10470 \[cs.LG\]](https://arxiv.org/abs/2108.10470).
- [34] M. T. Mason and K. M. Lynch, “Dynamic Manipulation,” in *IEEE/RSJ International Conference on Intelligent Robots and Systems (IROS)*, 1993.
- [35] J. Matas, S. James, and A. J. Davison, “Sim-to-Real Reinforcement Learning for Deformable Object Manipulation,” *Conference on Robot Learning (CoRL)*, 2018.
- [36] H. Mayer, F. Gomez, D. Wierstra, I. Nagy, A. Knoll, and J. Schmidhuber, “A System for Robotic Heart Surgery that Learns to Tie Knots Using Recurrent Neural Networks,” in *IEEE/RSJ International Conference on Intelligent Robots and Systems (IROS)*, 2006.
- [37] T. Morita, J. Takamatsu, K. Ogawara, H. Kimura, and K. Ikeuchi, “Knot Planning from Observation,” in *IEEE International Conference on Robotics and Automation (ICRA)*, 2003.
- [38] M. Mukadam, J. Dong, X. Yan, F. Dellaert, and B. Boots, “Continuous-time Gaussian Process Motion Planning via Probabilistic Inference,” in *International Journal of Robotics Research (IJRR)*, 2018.
- [39] A. Nair, D. Chen, P. Agrawal, P. Isola, P. Abbeel, J. Malik, and S. Levine, “Combining Self-Supervised Learning and Imitation for Vision-Based Rope Manipulation,” in *IEEE International Conference on Robotics and Automation (ICRA)*, 2017.
- [40] H. Nakagaki, K. Kitagi, T. Ogasawara, and H. Tsukune, “Study of Deformation and Insertion Tasks of Flexible Wire,” in *IEEE International Conference on Robotics and Automation (ICRA)*, 1997.
- [41] Y. Narang, Y. Li, M. Macklin, D. McConachie, and J. Wu, *RSS 2021 Workshop on Deformable Object Simulation in Robotics*, <https://sites.google.com/nvidia.com/do-sim>, Accessed: 2021-09-12.
- [42] D. Pathak, P. Mahmoudieh, G. Luo, P. Agrawal, D. Chen, Y. Shentu, E. Shelhamer, J. Malik, A. A. Efros, and T. Darrell, “Zero-Shot Visual Imitation,” in *International Conference on Learning Representations (ICLR)*, 2018.
- [43] X. B. Peng, M. Andrychowicz, W. Zaremba, and P. Abbeel, “Sim-to-Real Transfer of Robotic Control with Dynamics Randomization,” in *IEEE International Conference on Robotics and Automation (ICRA)*, 2018.
- [44] F. Ramos, R. Possas, and D. Fox, “Bayessim: Adaptive domain randomization via probabilistic inference for robotics simulators,” in *Proceedings of Robotics: Science and Systems*, Freiburg/Breisgau, Germany, Jun. 2019.
- [45] C. Rasmussen and C. Williams, *Gaussian Processes for Machine Learning*. MIT Press, 2006.

- [46] F. Ruiz-Ugalde, G. Cheng, and M. Beetz, "Fast adaptation for effect-aware pushing," in *2011 11th IEEE-RAS International Conference on Humanoid Robots*, IEEE, 2011, pp. 614–621.
- [47] F. Sadeghi and S. Levine, "CAD2RL: Real Single-Image Flight without a Single Real Image," in *Robotics: Science and Systems (RSS)*, 2017.
- [48] J. Sanchez, J.-A. Corrales, B.-C. Bouzgarrou, and Y. Mezouar, "Robotic Manipulation and Sensing of Deformable Objects in Domestic and Industrial Applications: a Survey," in *International Journal of Robotics Research (IJRR)*, 2018.
- [49] D. Seita, P. Florence, J. Tompson, E. Coumans, V. Sindhwani, K. Goldberg, and A. Zeng, "Learning to Rearrange Deformable Cables, Fabrics, and Bags with Goal-Conditioned Transporter Networks," in *IEEE International Conference on Robotics and Automation (ICRA)*, 2021.
- [50] S. Sen, A. Garg, D. V. Gealy, S. McKinley, Y. Jen, and K. Goldberg, "Automating Multi-Throw Multilateral Surgical Suturing with a Mechanical Needle Guide and Sequential Convex Optimization," in *IEEE International Conference on Robotics and Automation (ICRA)*, 2016.
- [51] B. Shahriari, K. Swersky, Z. Wang, R. P. Adams, and N. De Freitas, "Taking the human out of the loop: A review of bayesian optimization," *Proceedings of the IEEE*, vol. 104, no. 1, pp. 148–175, 2015.
- [52] Y. She, S. Dong, S. Wang, N. Sunil, A. Rodriguez, and E. Adelson, "Cable Manipulation with a Tactile-Reactive Gripper," in *Robotics: Science and Systems (RSS)*, 2020.
- [53] R. Storn and K. Price, "Differential evolution—a simple and efficient heuristic for global optimization over continuous spaces," *Journal of global optimization*, vol. 11, no. 4, pp. 341–359, 1997.
- [54] J. Tobin, R. Fong, A. Ray, J. Schneider, W. Zaremba, and P. Abbeel, "Domain Randomization for Transferring Deep Neural Networks from Simulation to the Real World," in *IEEE/RSJ International Conference on Intelligent Robots and Systems (IROS)*, 2017.
- [55] P. Virtanen, R. Gommers, T. E. Oliphant, M. Haberland, T. Reddy, D. Cournapeau, E. Burovski, P. Peterson, W. Weckesser, J. Bright, S. J. van der Walt, M. Brett, J. Wilson, K. J. Millman, N. Mayorov, A. R. J. Nelson, E. Jones, R. Kern, E. Larson, C. J. Carey, Í. Polat, Y. Feng, E. W. Moore, J. VanderPlas, D. Laxalde, J. Perktold, R. Cimrman, I. Henriksen, E. A. Quintero, C. R. Harris, A. M. Archibald, A. H. Ribeiro, F. Pedregosa, P. van Mulbregt, and SciPy 1.0 Contributors, "SciPy 1.0: Fundamental Algorithms for Scientific Computing in Python," *Nature Methods*, vol. 17, pp. 261–272, 2020.
- [56] C. Wang, S. Wang, B. Romero, F. Veiga, and E. Adelson, "Swing-Bot: Learning Physical Features from In-hand Tactile Exploration for Dynamic Swing-up Manipulation," in *IEEE/RSJ International Conference on Intelligent Robots and Systems (IROS)*, 2020.
- [57] G. Wang and N. Wereley, "Analysis of Fly Fishing Rod Casting Dynamics," *Shock and Vibration*, vol. 18, no. 6, pp. 839–855, 2011.
- [58] W. Wang and D. Balkcom, "Tying Knot Precisely," in *IEEE International Conference on Robotics and Automation (ICRA)*, 2016.
- [59] W. Wang, D. Berenson, and D. Balkcom, "An Online Method for Tight-Tolerance Insertion Tasks for String and Rope," in *IEEE International Conference on Robotics and Automation (ICRA)*, 2015.
- [60] Y. Wu, W. Yan, T. Kurutach, L. Pinto, and P. Abbeel, "Learning to Manipulate Deformable Objects without Demonstrations," in *Robotics: Science and Systems (RSS)*, 2020.
- [61] Y. Yamakawa, A. Namiki, and M. Ishikawa, "Motion Planning for Dynamic Knotting of a Flexible Rope With a High-Speed Robot Arm," in *IEEE/RSJ International Conference on Intelligent Robots and Systems (IROS)*, 2010.
- [62] —, "Simple Model and Deformation Control of a Flexible Rope Using Constant, High-speed Motion of a Robot Arm," in *IEEE International Conference on Robotics and Automation (ICRA)*, 2012.
- [63] —, "Dynamic High-Speed Knotting of a Rope by a Manipulator," in *International Journal of Advanced Robotic Systems*, 2013.
- [64] Y. Yamakawa, A. Namiki, M. Ishikawa, and M. Shimojo, "One-Handed Knotting of a Flexible Rope With a High-Speed Multi-fingered Hand Having Tactile Sensors," in *IEEE/RSJ International Conference on Intelligent Robots and Systems (IROS)*, 2007.
- [65] W. Yan, A. Vangipuram, P. Abbeel, and L. Pinto, "Learning Predictive Representations for Deformable Objects Using Contrastive Estimation," in *Conference on Robot Learning (CoRL)*, 2020.
- [66] A. Zeng, P. Florence, J. Tompson, S. Welker, J. Chien, M. Attarian, T. Armstrong, I. Krasin, D. Duong, V. Sindhwani, and J. Lee, "Transporter Networks: Rearranging the Visual World for Robotic Manipulation," in *Conference on Robot Learning (CoRL)*, 2020.
- [67] A. Zeng, S. Song, J. Lee, A. Rodriguez, and T. Funkhouser, "TossingBot: Learning to Throw Arbitrary Objects with Residual Physics," in *Robotics: Science and Systems (RSS)*, 2019.
- [68] H. Zhang, J. Ichnowski, D. Seita, J. Wang, and K. Goldberg, "Robots of the Lost Arc: Learning to Dynamically Manipulate Fixed-Endpoint Ropes and Cables," in *IEEE International Conference on Robotics and Automation (ICRA)*, 2021.
- [69] S. Zimmermann, R. Poranne, and S. Coros, "Dynamic Manipulation of Deformable Objects with Implicit Integration," in *IEEE Robotics and Automation Letters (RA-L)*, 2021.